Eur. Phys. J. B **1**, 173-177 (1998)

THE EUROPEAN PHYSICAL JOURNAL B

Effect of hydrodynamic flow on kinetics of nematic-isotropic transition in liquid crystals

J.-i. Fukuda[a]

Department of Physics, Kyoto University, Kyoto 606-01, Japan

Received: 8 September 1997 / Received in final form: 23 October 1997 / Accepted: 3 November 1997

Abstract. We investigate kinetics of nematic-isotropic transition by solving the hydrodynamic equations for the nematic 3×3 tensor order parameter $Q_{\alpha\beta}$ and the fluid velocity in two space dimension (x-y plane). Numerical results indicate that nematic directors tend to align parallel to the x-y plane when hydrodynamic flow is incorporated. Late stage growth exponents, $\phi_{\rm c}$ for the correlation length and $\phi_{\rm def}$ for the number of topological defects, are not significantly altered by hydrodynamic flow. However, in contrast to the case without flow, the relation $\phi_{\rm def} = -2\phi_{\rm c}$ holds well, which may indicate the validity of dynamical scaling for the case with hydrodynamic flow.

PACS. 64.70.Md Transitions in liquid crystals – 64.60.Cn Order-disorder transformations; statistical mechanics of model systems

Phase ordering kinetics of liquid crystal systems undergoing nematic-isotropic transition has attracted considerable experimental interest [1,2]. Liquid crystal systems can be characterized by a tensor order parameter [3], so they constitute a unique example of systems with continuous symmetry [4]. So far most of extensive theoretical [5,6] and numerical [7–10] efforts have been focused on vector models. Recently Zapotocky *et al.* [11] studied kinetics of uniaxial and biaxial nematic systems by numerically solving time-dependent Ginzburg-Landau equations which describe time evolution of a tensor order parameter without the velocity field. However, the hydrodynamic interaction often crucially influences phase transition kinetics. For example, it has been shown theoretically [12–14] and numerically [15–18] that hydrodynamic flow governs late stage phase separation kinetics in binary fluid mixtures. Here we note that little attention has been paid to the effect of hydrodynamic flow on systems with continuous symmetry. In this article we solve numerically the hydrodynamic equations of motion for the nematic 3×3 tensor order parameter in two space dimension and investigate the effect of hydrodynamic flow on the kinetics of the nematic-isotropic phase transition of a uniaxial nematic system, which has not been studied so far.

Hydrodynamic equations for the nematic order parameter $Q_{\alpha\beta}(\mathbf{r},t)$ and the fluid velocity $v_\alpha(\mathbf{r},t)$ were derived by Olmsted and Goldbart [19] to investigate the effect of shear on nematic-isotropic transition. We investigate here the effect of the flow induced by the stress due to molecular orientation, and we do not consider the situation with external flow like shear.

[a] e-mail: fukuda@ton.scphys.kyoto-u.ac.jp

We assume the incompressibility of the system and consider isothermal processes. The equation of motion for $Q_{\alpha\beta}(\mathbf{r},t)$ can be written as [19]

$$\left(\frac{\partial}{\partial t} + v_\gamma \partial_\gamma\right) Q_{\alpha\beta} + \kappa^{[\mathrm{a}]}_{\alpha\nu} Q_{\nu\beta} - Q_{\alpha\nu}\kappa^{[\mathrm{a}]}_{\nu\beta} = \beta_1 \kappa^{[\mathrm{s}]}_{\alpha\beta} + \frac{1}{\beta_2} H^{[\mathrm{s}]}_{\alpha\beta} + \theta^Q_{\alpha\beta}, \tag{1}$$

where Greek indices represent x, y and z and $\partial_\alpha \equiv \partial/\partial x_\alpha$. $\kappa_{\alpha\beta} \equiv \partial_\alpha v_\beta$ is the velocity gradient tensor and $H_{\alpha\beta} \equiv -\delta F\{Q_{\alpha\beta}\}/\delta Q_{\alpha\beta}$ is the molecular field, $F\{Q_{\alpha\beta}\}$ being the free energy of the system which will be given later. β_1 and β_2 are transport coefficients. $\theta^Q_{\alpha\beta}$ is a thermal noise satisfying the fluctuation-dissipation theorem. The superscripts [s] and [a] denote the symmetric-traceless part and the antisymmetric part of a second-rank tensor, respectively. Hereafter summations over repeated indices are implied. The equation of motion for $v_\alpha(\mathbf{r},t)$ is

$$\rho\left(\frac{\partial}{\partial t} + v_\gamma \partial_\gamma\right) v_\alpha = \partial_\gamma \sigma_{\gamma\alpha} + \theta^v_\alpha, \tag{2}$$

$$\partial_\alpha v_\alpha = 0, \tag{3}$$

where ρ is the density and a thermal noise term θ^v_α satisfies the fluctuation-dissipation theorem. Equation (3) represents the incompressibility of the fluid. The total stress tensor $\sigma_{\alpha\beta}$ can be expressed as $\sigma_{\alpha\beta} = \sigma^{i[\mathrm{s}]}_{\alpha\beta} + \sigma^{i[\mathrm{a}]}_{\alpha\beta} + \sigma^{\mathrm{d}}_{\alpha\beta} - p\delta_{\alpha\beta}$, where $\sigma^{i[\mathrm{s}]}_{\alpha\beta}$, $\sigma^{i[\mathrm{a}]}_{\alpha\beta}$ and $\sigma^{\mathrm{d}}_{\alpha\beta}$ are the irreversible symmetric (dissipative) part, the irreversible antisymmetric

(torque) part and the distortion part, respectively and are given by

$$\sigma^{i[\mathrm{s}]}_{\alpha\beta} = \beta_3 \kappa^{[\mathrm{s}]}_{\alpha\beta} - \beta_1 H^{[\mathrm{s}]}_{\alpha\beta}, \tag{4}$$

$$\sigma^{i[\mathrm{a}]}_{\alpha\beta} = H^{[\mathrm{s}]}_{\alpha\nu} Q_{\nu\beta} - Q_{\alpha\nu} H^{[\mathrm{s}]}_{\nu\beta}, \tag{5}$$

$$\sigma^{\mathrm{d}}_{\alpha\beta} = -\frac{\delta F}{\delta(\partial_\alpha Q_{\mu\nu})} \partial_\beta Q_{\mu\nu}. \tag{6}$$

The isotropic pressure part $-p\delta_{\alpha\beta}$ ensures the incompressibility condition. β_3 in equation (4) is a third transport coefficient, and the same coefficient β_1 appears in equations (1, 4) to satisfy the Onsager reciprocal theorem [19]. Olmsted and Goldbart [19] neglected the dependence of β_1, β_2, and β_3 on the order parameter $Q_{\alpha\beta}$, because they considered the situation close to a weakly first-order transition point with small $Q_{\alpha\beta}$. We also treat them simply as constants, although hereafter we consider a situation where isotropic states become unstable and $Q_{\alpha\beta}$ is not necessarily small.

The free energy F is the sum of the Landau-de Gennes free energy F_{L} and the distortion energy F_{d}. F_{L} is given by the power series expansion in $Q_{\alpha\beta}$ up to fourth order and can be presented as [3]

$$F_{\mathrm{L}} = \int \mathrm{d}\mathbf{r} \left(\frac{1}{2} A Q_{\alpha\beta} Q_{\alpha\beta} + \frac{1}{3} B Q_{\alpha\beta} Q_{\beta\gamma} Q_{\gamma\alpha} + \frac{1}{4} C (Q_{\alpha\beta} Q_{\alpha\beta})^2 \right). \tag{7}$$

Let us suppose the case, $A < 0$, where the isotropic state with $Q_{\alpha\beta} = 0$ becomes unstable. F_{d} can be taken to be

$$F_{\mathrm{d}} = \int \mathrm{d}\mathbf{r} \left(\frac{1}{2} L_1 \partial_\alpha Q_{\beta\gamma} \partial_\alpha Q_{\beta\gamma} + \frac{1}{2} L_2 \partial_\alpha Q_{\alpha\beta} \partial_\gamma Q_{\gamma\beta} \right), \tag{8}$$

where L_1 and L_2 are elastic moduli. When $L_2 = 0$, rotations of the reference frame and orthogonal transformation of the order parameter tensor are uncorrelated,which greatly simplifies calculations. For instance, molecular field due to F_{d} becomes $-\delta F_{\mathrm{d}}/\delta Q_{\alpha\beta} = L_1 \nabla^2 Q_{\alpha\beta}$. That is, the choice $L_2 = 0$ yields the one constant approximation ($K_1 = K_2 = K_3$) in the Frank elastic energy [3]. It should also be noted that if we take $L_2 = 0$, no anisotropy appears in F_{d} and $H_{\alpha\beta}$ even in a two-dimensional system where the derivative with respect to z is not considered ($\partial_z = 0$). Thus we consider the situation $L_2 = 0$ hereafter.

We numerically integrate equations (1, 2) in the Euler scheme on a two-dimensional 256×256 square lattice with the periodic boundary conditions. We take the x-y plane as the plane of the system and we assume $v_z = 0$ and $\partial_z = 0$, supposing a thin film system. We emphasize that $Q_{\alpha\beta}$ is a 3×3 tensor, not a 2×2 tensor. It implies that directors can point to any direction in three-dimensional space, although we consider two-dimensional systems. We also assume the Stokes approximation $0 \simeq \rho(\partial/\partial t + v_\gamma \partial_\gamma) v_\alpha = \partial_\gamma \sigma_{\gamma\alpha}$ as is usual for liquid crystals.

In all our simulations we set $A = -4.5, B = -6, C = 5, L_1 = 0.5, L_2 = 0$, $\beta_1 = \beta_2 = 1, \Delta x = 0.5$, and $\Delta t = 0.05$. β_3 is set to 2, 5 or 20. When we take smaller β_3, v_α becomes larger and fluid flow becomes more important. As the initial condition at $t = 0$, $Q_{\alpha\beta}$ at each lattice point are random numbers uniformly distributed in $[-0.02, 0.02]$ satisfying $Q_{\alpha\alpha} = 0$ and $Q_{\alpha\beta} = Q_{\beta\alpha}$. Thermal fluctuation is incorporated only in the initial conditions and $\theta^Q_{\alpha\beta}$ and θ^v_α in equations (1, 2) are neglected in our simulations.

In Figure 1 we show time evolution of the Schlieren patterns for the hydrodynamic case with $\beta_3 = 2$ and the purely dissipative case without hydrodynamic flow ($\partial Q_{\alpha\beta}/\partial t = (1/\beta_2) H^{[\mathrm{s}]}_{\alpha\beta}$). Larger Q^2_{xy} is clearly observed in the hydrodynamic case, indicating that directors have a remarkable tendency to align parallel to the x-y plane. To see more quantitatively, we show in Figure 2 time evolution of the spatial and statistical average $\langle Q_{\alpha\beta} \rangle$. Statistical average is taken over 50 independent runs. We can see that $\langle Q_{\alpha\beta} \rangle$ acquires a finite value in the case with hydrodynamic flow, while $\langle Q_{\alpha\beta} \rangle$ remains zero without hydrodynamic flow. We also find that in the case with hydrodynamic flow, $\langle Q_{xx} \rangle$, $\langle Q_{yy} \rangle$ and $\langle Q_{zz} \rangle$ approach 0.25, 0.25 and -0.5, respectively, while $\langle Q_{xy} \rangle$, $\langle Q_{yz} \rangle$ and $\langle Q_{xz} \rangle$ remain zero. This result can be understood by the following arguments: F_{L} given in equation (7) acquires its minimum when

$$Q_{\alpha\beta} = \frac{3}{2} S \left(n_\alpha n_\beta - \frac{1}{3} \delta_{\alpha\beta} \right), \tag{9}$$

where n_α is a unit vector of arbitrary direction and S is a positive solution of $2A + BS + 3CS^2 = 0$ when $A, B < 0$. If we take the average of equation (9) with the condition that $n_z = 0$ and n_α can point to any direction isotropically in the x-y plane, we obtain

$$\begin{aligned} \langle Q_{xx} \rangle = \langle Q_{yy} \rangle &= \frac{1}{4} S, \\ \langle Q_{zz} \rangle &= -\frac{1}{2} S, \\ \langle Q_{xy} \rangle = \langle Q_{yz} \rangle = \langle Q_{xz} \rangle &= 0. \end{aligned} \tag{10}$$

For the parameters in our simulations, $S = 1$ and equation (10) coincides with our numerical results.

To confirm the above tendency analytically, we perform a linear stability analysis of the isotropic state $Q_{\alpha\beta} = 0$. The fluid velocity v_α can be represented in terms of $Q_{\alpha\beta}$ under the Stokes approximation, and the equation of motion (1) becomes, up to linear order in $Q_{\alpha\beta}$,

$$\begin{aligned} \frac{\partial}{\partial t} Q_{\alpha\beta}(\mathbf{q}) &\simeq \Lambda_{\alpha\beta\mu\nu}(\mathbf{q}) \frac{1}{\beta_2} H^{[\mathrm{s}]}_{\mu\nu} \\ &\simeq -\Lambda_{\alpha\beta\mu\nu}(\mathbf{q}) \frac{1}{\beta_2} (A + L_1 q^2) Q_{\mu\nu}(\mathbf{q}), \end{aligned} \tag{11}$$

where $Q_{\alpha\beta}(\mathbf{q})$ is the Fourier transform of $Q_{\alpha\beta}(\mathbf{r})$, $\mathbf{q}$ being the wavenumber. Note that $L_2 = 0$ is assumed again in

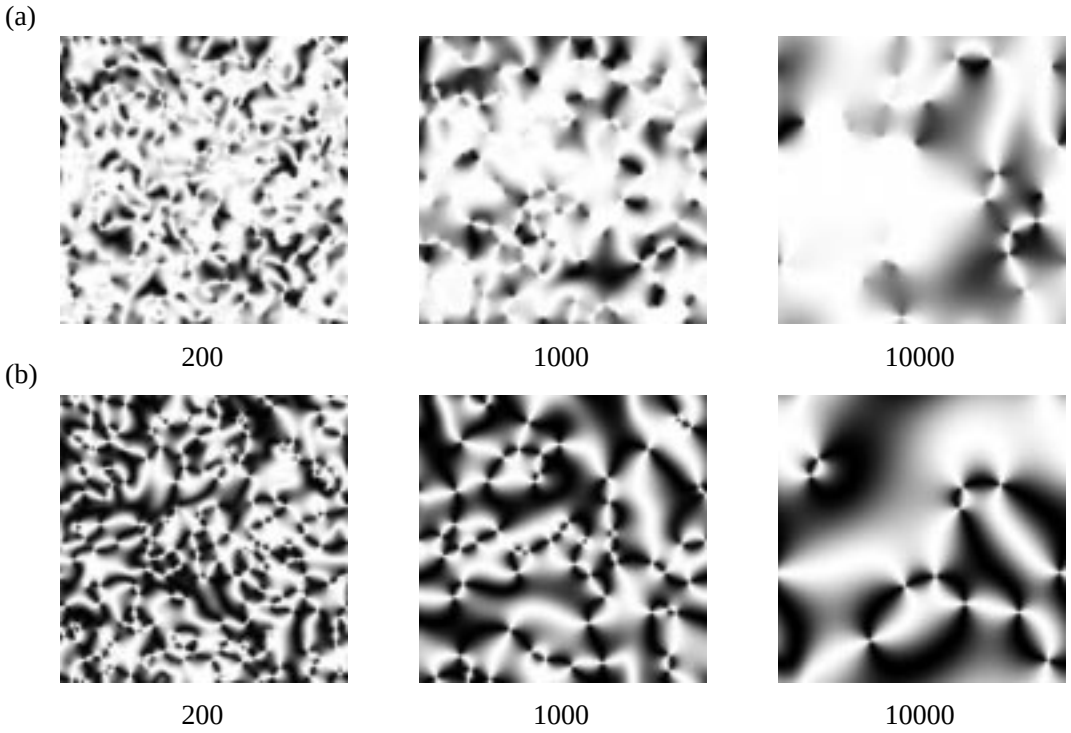

Fig. 1. Schlieren patterns obtained for (a) the purely dissipative case and (b) the hydrodynamic case ($\beta_3 = 2$). Darkness represents Q_{xy}^2. The numbers are the time steps. Under the same initial conditions.

the second line of equation (11). The tensor $\Lambda_{\alpha\beta\mu\nu}(\mathbf{q})$ is given by

$$\Lambda_{\alpha\beta\mu\nu}(\mathbf{q}) = \delta_{\alpha\mu}\delta_{\beta\nu} + \frac{\beta_1^2\beta_2}{\beta_3 q^4} q_\mu \{q_\alpha(q^2\delta_{\beta\nu} - q_\beta q_\nu) + q_\beta(q^2\delta_{\alpha\nu} - q_\alpha q_\nu)\}. \quad (12)$$

$\Lambda_{\alpha\beta\mu\nu}$ is essentially a 5×5 matrix because $Q_{\alpha\beta}$ is symmetric and traceless and has only 5 independent components. Calculation of the eigenmodes of the tensor $\Lambda_{\alpha\beta\mu\nu}$ is straightforward and under the condition $q_z = 0$ (which implies $\partial_z = 0$) and $v_z = 0$, it can be shown that four out of the five eigenmodes have the eigenvalue 1, and that the rest eigenmode

$$(Q_{xx} - Q_{yy}, Q_{xy}, Q_{xz}, Q_{yz}, Q_{zz}) \propto (4q_x q_y, q_y^2 - q_x^2, 0, 0, 0) \quad (13)$$

has the eigenvalue

$$\lambda = 1 + (\beta_1^2\beta_2/\beta_3), \quad (14)$$

greater than 1 and independent of the wavenumber $\mathbf{q}$. We can see from equation (14) that λ becomes large with large β_2 and small β_3. β_2 is proportional to the relaxation time of the orientational order (without flow) and β_3 corresponds to the viscosity of the fluid. Therefore the effect of hydrodynamic flow becomes more pronounced when orientational order relaxes more slowly and the fluid is less viscous. We emphasize that hydrodynamic correction can be crucial. In fact, we estimate $\lambda \simeq 9$ using the parameters of MBBA, $\beta_1 = 0.9$ and $\beta_3 \simeq 0.1\beta_2$ [19]. In our simulations we used a larger value $\beta_3 = 2(= 2\beta_2)$ to avoid numerical instability. Equation (13) implies that the mode which grows fastest is parallel to the x-y plane. Without hydrodynamic flow and with $L_2 = 0$, neither the free energy F nor the equation of motion $\partial Q_{\alpha\beta}/\partial t = (1/\beta_2)H_{\alpha\beta}^{[s]}$ prefers any direction and thus the statistical average $\langle Q_{\alpha\beta}\rangle$ should be zero. This does not imply that the spatial average of $Q_{\alpha\beta}$ for one system ($\overline{Q_{\alpha\beta}}$) should be zero; $\overline{Q_{\alpha\beta}} \neq 0$ due to spontaneous symmetry breaking. On the other hand, hydrodynamic flow breaks the symmetry of the dynamics as discussed above. Therefore $\langle Q_{\alpha\beta}\rangle$ becomes non-zero for the hydrodynamic case.

To check how late stage dynamics is modified by hydrodynamic flow, we calculate from our numerical results the correlation length $L(t)$ and the number of defects $N(t)$. For the definition of $L(t)$, we use the correlation function for the order parameter defined by

$$C(\mathbf{r}, t) = \left\langle \frac{\int d\mathbf{r}'(Q_{\alpha\beta}(\mathbf{r}', t) - Q_{\alpha\beta}^0)(Q_{\alpha\beta}(\mathbf{r}' + \mathbf{r}, t) - Q_{\alpha\beta}^0)}{\int d\mathbf{r}'(Q_{\alpha\beta}(\mathbf{r}', t) - Q_{\alpha\beta}^0)^2} \right\rangle. \quad (15)$$

For the hydrodynamic case we take $Q_{xx}^0 = Q_{yy}^0 = 1/4$, $Q_{zz}^0 = -1/2$, and $Q_{xy}^0 = Q_{yz}^0 = Q_{xz}^0 = 0$, and for the purely dissipative case $Q_{\alpha\beta}^0 = 0$. It follows from the definition that $C(0, t) = 1$. We define $L(t)$ through $C(L(t), t) = 1/2$.

We show the time dependence of $L(t)$ and $N(t)$ in Figure 3 for the purely dissipative case and the hydrodynamic cases with $\beta_3 = 2, 5$ and 20. We also calculate the growth

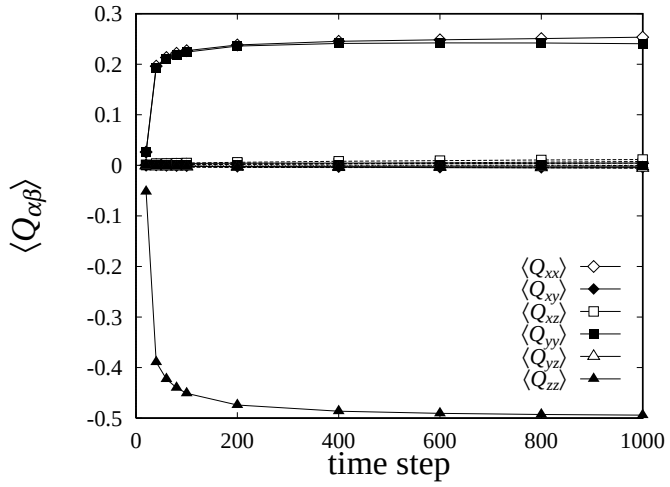

Fig. 2. Time evolution of $\langle Q_{\alpha\beta}\rangle$ for the hydrodynamic case with $\beta_3 = 2$ (solid lines) and for the purely dissipative case (dashed lines). Average is taken over 50 independent runs. Symbols are common to both cases.

exponents, ϕ_c for $L(t)$ and ϕ_{def} for $N(t)$, defined by

$$L(t) \sim t^{\phi_c}, \\ N(t) \sim t^{\phi_{def}}. \tag{16}$$

For the purely dissipative case $\phi_c = 0.402 \pm 0.002$ and $\phi_{def} = -0.751 \pm 0.005$, which reproduces the results obtained by Zapotocky *et al.* [11] For the hydrodynamic cases $\phi_c = 0.432 \pm 0.002$ and $\phi_{def} = -0.868 \pm 0.005$ for $\beta_3 = 2$, $\phi_c = 0.428 \pm 0.002$ and $\phi_{def} = -0.845 \pm 0.004$ for $\beta_3 = 5$ and $\phi_c = 0.402 \pm 0.003$ and $\phi_{def} = -0.809 \pm 0.002$ for $\beta_3 = 20$. All the exponents are calculated by using the data from 500 to 8000 time steps. We find that hydrodynamic flow only slightly fastens the transition kinetics.

Here we make a comment on the relation between these two exponents ϕ_c and ϕ_{def}. If dynamical scaling holds and a single length scale $L(t)$ can characterize the late stage property of the phase transition kinetics, $N(t)$ should behave as $N(t) \sim L(t)^{-2}$, hence

$$\phi_{def} = -2\phi_c, \tag{17}$$

for the two-dimensional system we consider. For the case without hydrodynamic flow equation (17) does not hold and dynamical scaling hypothesis is violated in spite of the good collapse of the scaled correlation functions [11]. On the contrary, equation (17) holds well for the hydrodynamic cases. It may show, together with a good collapse of the scaled correlation functions $C(r/L(t), t)$ shown in Figure 4, that dynamical scaling holds for the hydrodynamic cases.

To see why hydrodynamic flow does not significantly affect the late stage phase transition kinetics, velocity profile shown in Figure 5 may be helpful. This indicates that in the late stage fluid flow is important only in the vicinity of the topological defects. In the nematic systems we consider, topological defects are points in two dimensions

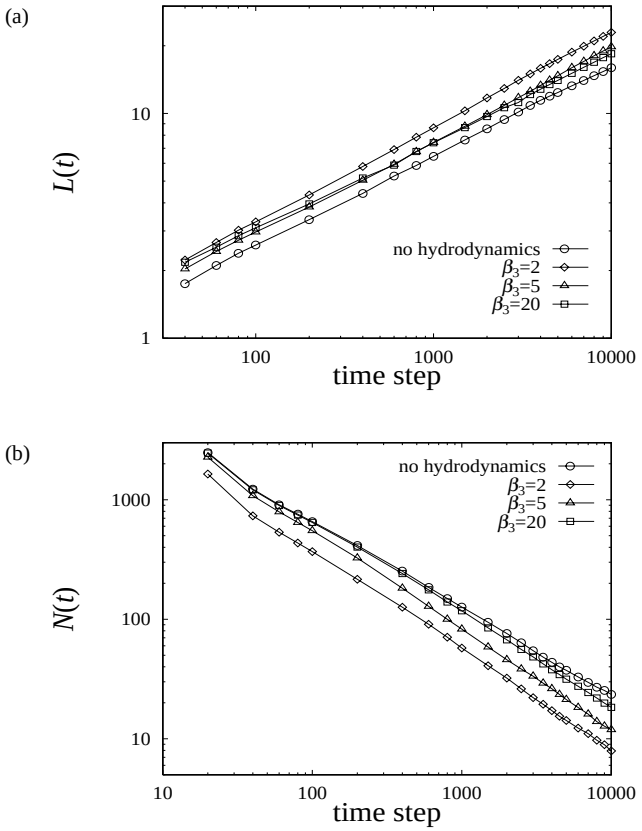

Fig. 3. Time evolution of (a) the correlation length $L(t)$ and (b) the number of defects $N(t)$.

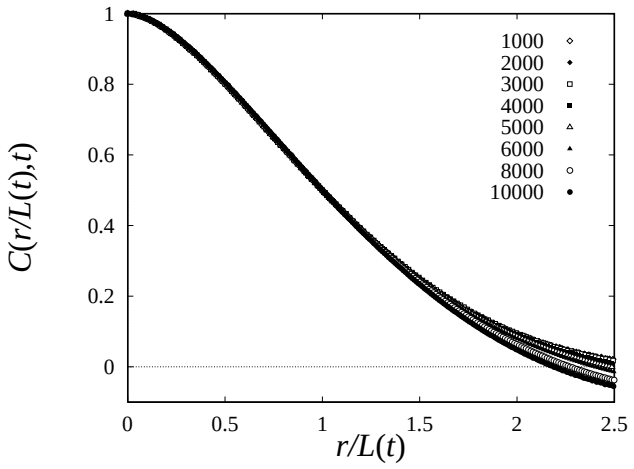

Fig. 4. Scaled correlation functions $C(r/L(t), t)$ for the hydrodynamic case with $\beta_3 = 2$. The numbers are the time steps. Average is taken over 50 independent runs. A good collapse on a single master curve is observed except for the tail.

(lines in three dimensions) and are not expected to induce fluid flow when distances between defects are long. In binary fluid mixtures, in contrast, fluid flow is induced by lines in two dimension (surfaces in three dimensions) and thus greatly affects the late stage kinetics [12,13]. We also note that the effective kinetic coefficient $\Lambda_{\alpha\beta\mu\nu}(\mathbf{q})/\beta_2$ appearing in the linearized equation of motion (11)

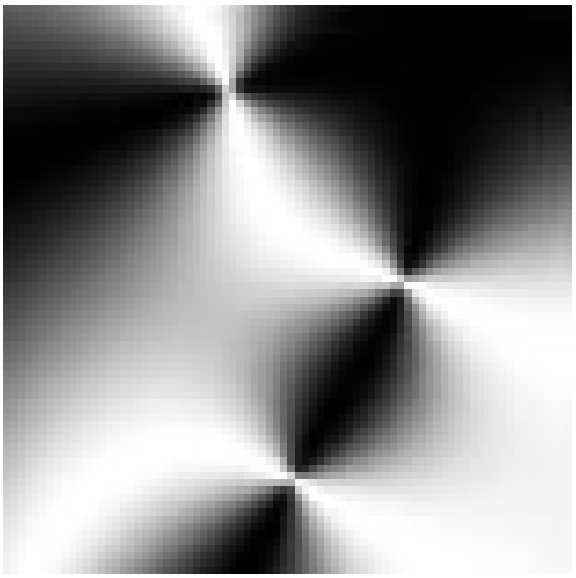

(a)

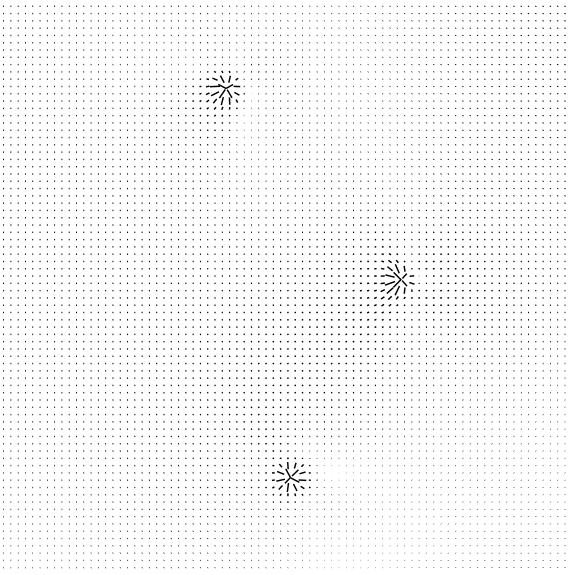

(b)

Fig. 5. 78×78 portions of the Schlieren pattern (a) and the corresponding velocity profile (b) at 15000 time step for $\beta_3 = 2$. Note that fluid flow is important only in the vicinity of the topological defects.

depends only on the orientation of the wavevector $\mathbf{q}$ and is independent of the magnitude of $\mathbf{q}$. This implies that hydrodynamic flow gives a marginal contribution to the dynamics, which is essentially independent of the length scale characterizing the late stage properties of the phase transition kinetics.

In summary, we have investigated the phase ordering kinetics of uniaxial liquid crystal systems undergoing nematic-isotropic transition by numerically solving the equations of motion for the orientational 3×3 tensor order parameter and the fluid flow in two dimensions. The statistical average of the order parameter acquires a finite value in contrast to the case without hydrodynamic flow, which indicates that hydrodynamic flow induces the orientational order parallel to the plane of the system. This can be understood by the linear stability analysis of an isotropic state, which shows that one of the modes grows faster than the others due to hydrodynamic flow, leading to the asymmetry of the kinetics. In the late stage, the fluid flows do not affect remarkably the coarsening kinetics. However, when hydrodynamic flow is incorporated, the relation between the growth exponents $\phi_{\rm def} = -2\phi_{\rm c}$ holds well in contrast to the case without flow. This relation together with a good collapse of the scaled correlation functions may indicate that dynamical scaling holds for the hydrodynamic cases.

The author is grateful to Professor Akira Onuki, Professor Shigeyuki Komura and Dr. Ryoichi Yamamoto for helpful discussion and critically reading this manuscript. Thanks are also due to Professor Yasuhiro Shiwa, Professor Toshihiro Kawakatsu and Dr. Takashi Taniguchi for useful comments.

References

1. A.P.Y. Wong, P. Wiltzius, B. Yurke, Phys. Rev. Lett. **68**, 3583 (1992); A.P.Y. Wong, P. Wiltzius, R.G. Larson, B. Yurke, Phys. Rev. E **47**, 2683 (1993).
2. I. Chuang, B. Yurke, A.N. Pargellis, Phys. Rev. E **47**, 3343 (1993).
3. P.G. de Gennes, J. Prost, *The Physics of Liquid crystals 2nd edition* (Oxford University Press, 1993).
4. For a review, see A.J. Bray, Physica A **194**, 41 (1993).
5. H. Toyoki, Phys. Rev. B **45**, 1965 (1992).
6. R.E. Blundell, A.J. Bray, Phys. Rev. E **49**, 4925 (1994).
7. Mondello M., Goldenfeld N., Phys. Rev. A **42**, 5865 (1990); *ibid.* **45**, 657 (1992).
8. R.E. Blundell, A.J. Bray, Phys. Rev. A **46**, R6154 (1992).
9. B. Yurke, A.N. Pargellis, T. Kovacs, D.A. Huse, Phys. Rev. E **47**, 1525 (1993).
10. H. Toyoki, Phys. Rev. E **47**, 2558 (1993).
11. M. Zapotocky, P.M. Goldbart, N. Goldenfeld, Phys. Rev. E **51**, 1216 (1995).
12. E.D. Siggia, Phys. Rev. A **20**, 595 (1979).
13. K. Kawasaki, T. Ohta, Physica A **118**, 175 (1983).
14. H. Furukawa H., Phys. Rev. A **31**, 1103 (1985); Physica A **204**, 237 (1994).
15. J.E. Farrell, O.T. Valls, Phys. Rev. B **40**, 7027 (1989); *ibid.* **42**, 2353 (1990); O.T. Valls, J.E. Farrell, Phys. Rev. E **47**, R36 (1993).
16. T. Koga, K. Kawasaki, Phys. Rev. A **44**, R817 (1991); Physica A **196**, 389 (1993).
17. S. Puri, B. Dünweg, Phys. Rev. A **45**, R6977 (1992).
18. Y. Wu, F.J. Alexander, T. Lookman, S. Chen, Phys. Rev. Lett. **74**, 3852 (1995).
19. P.D. Olmsted, P.M. Goldbart, Phys. Rev. A **41**, 4578 (1990); *ibid.* **46**, 4966 (1992).